Camera-based model to predict the total difference between effect coatings under directional illumination

Zhongning Huang (黄中宁)[1,2], Haisong Xu (徐海松)[1*], and M. Ronnier Luo[2]

[1]*State Key Laboratory of Modern Optical Instrumentation, Zhejiang University, Hangzhou 310027, China*

[2]*Department of Color Science, University of Leeds, Leeds LS2 9JT, UK*

[*]*Corresponding author: chsxu@zju.edu.cn*

Received January 24, 2011; accepted March 31, 2011; posted online June 21, 2011

A camera-based model is established to predict the total difference for samples of metallic panels with effect coatings under directional illumination, and the testing results indicate that the model can precisely predict the total difference between samples with metallic coatings with satisfactory consistency to the visual data. Due to the limited amount of testing samples, the model performance should be further developed by increasing the training and testing samples.

OCIS codes: 330.1690, 330.1710, 330.1715, 330.1730.

doi: 10.3788/COL201109.093301.

Products with effect coatings have unique characteristics, i.e., large change in appearance (color, glint, and coarseness) under different viewing conditions. The traditional methods of characterizing this kind of coatings can only assess their color or the gloss level based on the standard illumination and observation conditions recommended by commission internationale de edairage (CIE) or international standard organization (ISO) without judging the glint or the coarseness effect of them, which is quite far from the fact and cannot meet the demand of online quality control in industries[1,2]. Hence, further studies have become necessary and urgent due to the growing number of products with effect coatings and the increasing amount of metallic coatings produced by pigment manufacturers[3,4].

Metallic coatings are the most common and oldest effect coatings used in modern industries[3−6]. In contrast to conventional solid coatings, the chromaticity and lightness of metallic coatings strongly depend on illumination and viewing geometry, thus the metallic coatings can accentuate the curved profile of an object, which helps in attracting consumers via the amazing appearance. Traditional instrumental methods for their characterization always include multi-angle or multi-geometry measurement and concentrate on the angle dependence of the color. These methods, however, ignored texture properties that might affect the appearance of effect coatings heavily. For this reason, a camera-based model, that could assess effective samples in terms of the total difference, including color difference and glint difference, was proposed in this study.

It has been found from the experience of industry applications that effective pigments affect not only the color but also another aspect of coating appearance, namely the visual texture[5−7]. Visual texture is the perceived small-scale non-uniformity of the color when observed within a distance of a meter or less. It is an important property for its contribution to the overall appearance of effect coatings. Under directional illumination, glint, belonging to the scope of visual texture, is considered as the most important attribute influencing the overall appearance of effective pigments. It is defined as the tiny spot that is strikingly brighter than its surrounding and only visible under directional illumination conditions. The glint effect would change when the observation geometry is altered, hence it is angle dependent. Glint value is supposed to correlate with the local contrast between the bright sparkle and its surrounding, and the amount of sparkles as well. In this letter, a camera-based model to predict the total difference for samples of metallic panels with metallic coatings under directional illumination was established.

The statistics of model performance was evaluated in this study in terms of standardized residual sum of squares (STRESS)[8], which is calculated by

$$\mathrm{STRESS} = \left(\frac{\sum (\Delta E_i - F\Delta V_i)^2}{\sum F^2 \Delta V_i^2} \right)^{1/2} \times 100, \qquad (1)$$

where i is the index, ΔE_i and ΔV_i are two groups of data, and F always equals 1 since ΔE_i and ΔV_i have the same unit in this study. Evidently, the STRESS value will be 0 if the two groups of data are exactly the same. The STRESS will increase with the rise in the difference between the two groups.

The visual experiment was completed and illustrated in the authors' previous paper[9], thus the focus in this study is on the algorithm to predict the total difference of sample pairs via images of physical samples based on a digital camera. The framework of this model is given in Fig. 1. The images of samples were taken by the digital camera NIKON D80 in the same viewing geometry with the visual experiment under directional illumination, as shown in Fig. 2, to make sure that the samples could be precisely represented in the captured images.

The camera was set with f-number (F) of 6.3 and exposure time of 1/40 s. The captured images were 3 872×2 592 pixels, with both the vertical and horizontal resolution being 300 dpi. The central 1 000×1 000 pixels of the images, corresponding to the central area of the samples, were chosen for further image analysis.

In a perfect imaging system, the camera response is supposed to have a linear relationship with the incident

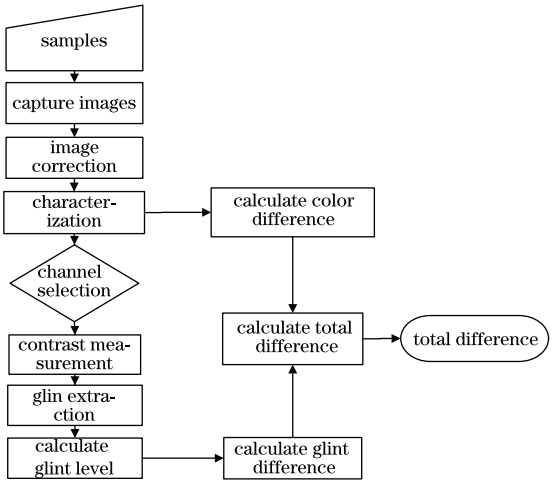

Fig. 1. Flowchart of the main framework for the total difference model under directional illumination.

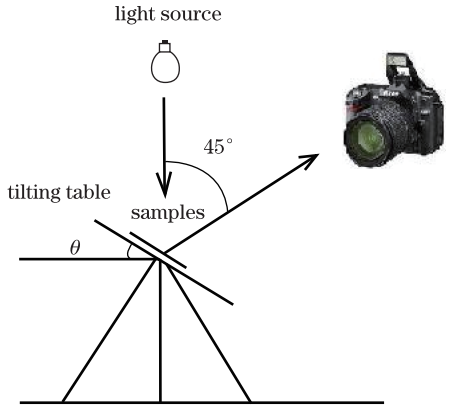

Fig. 2. Geometry for image capture under directional illumination with θ being 58°.

energy. However, the real commercial camera response would always be corrected as

$$dRGB = RGB^{\gamma}, \tag{2}$$

where $dRGB$ is the charge-coupled device (CCD) responses of red (R), green (G), and blue (B) channels, γ is a constant, and RGB is the camera output. There were six neutral colors in the GretagMacbeth ColorChecker Color Rendition Chart. In this study, five neutral colors, four of which were grey and one was black, were utilized to linearize the camera response, and the remaining neutral color with the highest reflectance was eliminated because it exceeds the dynamic range of the camera when being imaged under the experimental condition. This linearization procedure was achieved via two steps. Firstly, the mean RGB values of each image for the charts were normalized by dividing the largest RGB values of the five colors, namely rgb, and the sum of spectral power distribution (SPD) T, obtained by summing the SPD of the corresponding samples, which was also normalized as t by dividing the corresponding largest T value, resulting in the data of Table 1. Secondly, taking rgb for the abscissa and t for the longitudinal, the transformation function between the normalized camera output rgb and the linearized $lRGB$ could be determined as

$$lRGB = \alpha \times rgb^{\beta}, \tag{3}$$

where rgb is the normalized camera response, $lRGB$ is the linearized RGB, and α and β are both constants, as listed in Table 2, where R^2 is statistic using uppercase to quantify goodness of fit.

The intensity of the illumination was not uniform over the capturing field due to the spot light source used. In addition, in the context of the camera, the spatial uniformity correction was assumed to compensate for any non-uniformity in the sensitivity of each individual element of a CCD array and imperfection in an optical system. Due to the non-uniformity of the captured image, the original image of a uniform white paper without fluorescent effect over the viewing field showed that the sum of the R, G, and B channels ranged from 609 to 705. The spatial correction in this study was performed in R, G, and B channels, respectively, by the adoption of the Hardeberg's method[10] as

$$Q(i,j) = \frac{(lRGB_{\mathrm{w}} - lRGB_{\mathrm{d}}) \times [lRGB(i,j) - lRGB_{\mathrm{d}}(i,j)]}{[lRGB_{\mathrm{w}}(i,j) - lRGB_{\mathrm{d}}(i,j)]}, \tag{4}$$

where $lRGB$ (i, j) is the linearized camera response for either red, green, or blue channel of the images at pixel position (i, j); $lRGB_{\mathrm{w}}$ and $lRGB_{\mathrm{d}}$ are the mean linearized camera responses of the uniform white and uniform black, respectively; and $Q(i, j)$ is the RGB value after the spatial correction.

In order to obtain the color parameters of the samples from their images, colorimetric characterization must be carried out for the digital camera, which was realized by the polynomial regression model with least-square fitting[11−13]. To determine the optimized augmented matrix to transfer the linearized $lRGB$ into CIE tristimulus values XYZ, various augmented matrices with different sizes were tested in this study to investigate their suitability, as shown in Table 3.

Table 1. The Sum of SPD and the Camera Response of the Five Neutral Colors for the GretagMacbeth ColorChecker Color Rendition Chart

Grey Level	T	t	R	G	B	r	g	b
1	0.358	1.000	252.427	235.666	168.940	1.000	1.000	1.000
2	0.219	0.614	221.476	204.179	136.517	0.877	0.866	0.808
3	0.112	0.314	187.367	173.193	104.799	0.742	0.735	0.620
4	0.055	0.155	122.868	107.776	45.763	0.487	0.457	0.271
5	0.024	0.068	74.649	63.361	18.940	0.296	0.269	0.112

Table 2. The α and β Values of R, G, and B Channels and the Corresponding R^2

Channels	α	β	R^2
Red	0.7891	2.1215	0.9637
Green	0.7840	1.9589	0.9607
Blue	0.7643	1.1620	0.9554

For the camera characterization, an increase in the amount of training samples could improve the characterization accuracy. Due to the limited amount of available samples for this study, 44 of the 50 samples were used as training samples and the remaining 6 as testing samples. The characterization accuracy was evaluated in terms of color difference in CIELAB, as listed in Table 4. When the size of the transfer matrix was 3×20, the mean characterization accuracy was 1.09 CIELAB unit, which was very close to the just notice difference of 1.0 CIELAB unit[6]. Although the accuracy was even better when using the transfer matrix of 3×35, it was more likely to involve distortion due to the use of the high-order term of the RGB values[11−13]. Thus, the transfer matrix of 3×20 was employed to perform the colorimetric characterization of the digital camera. With the transfer matrix of 3×20, the characterization model accuracy with a different balance between the training and testing samples was also evaluated. The characterization accuracy in terms of CIELAB color difference were 1.12, 3.28, and 4.17 with the ratio of training and testing samples being 40:10, 30:20, and 25:25, respectively. It was evident that the accuracy was not acceptable if the training samples were less than 40 because of the rapid growth of characterization error. Moreover, when the amount of training samples was 44, the characterization model accuracy was very close to 1 CIELAB color difference, suggesting that the balance of training and testing samples adopted in this study is reasonable.

Through the characterization model described above, the images were transformed from the device-dependent RGB space into the device-independent XYZ. The human vision system is more sensitive to the luminance than to either the chroma or hue; even when watching a colored object, the observer could only see the luminance properties for the spots with high level of luminance. Hence, the luminance channel Y was chosen to extract the glint characteristic.

During the visual experiment, observers were informed that the glint value was determined by local contrast between the bright sparkle and its surrounding, together with the amount of sparkles. The local contrast could be obtained by subtracting the background from the images, and the amount of sparkles could be directly counted in the images. However, it was found after further analysis that the minimum luminance value of some yellow samples was bigger than the maximum of some of the dark samples, while the glint value was less than that of the dark samples, according to the observer's opinion. Herewith, it was necessary to eliminate the background effect when quantizing the glint, which was realized by subtracting the mode of the corresponding luminance image. This mode was the Y value that occurred with the highest frequency in the image, thus it represented the luminance value of the background in the image.

Image segmentation was implemented in order to separate the image into two regions: spots and background. Similar to the solid color, the distribution of the background of the samples was a bell-shaped symmetric histogram with most of the frequency counts bunched in the middle and with the counts dying out in the tails[7]. This implied that the frequency counts would die out at the critical value t, as shown in Fig. 3, if there is no metallic coating on the sample surface. Thus, it is reasonable to utilize the distribution estimation method to realize image segmentation[7]. As illustrated in Fig. 3, p is the corresponding mode of each individual image, l is the minimum pixel value of the corresponding image, and t with its value of $2p-l$ is the critical value to distinguish between the background and the glint spots.

The statistical approach proposed to extract glint characteristics correlated with the measured glint value using the BYK mac is as[7]

$$\text{Glint} = \alpha \times \log_{10}\left\{\frac{\sum_{\text{mean}}[\text{particle}(Y(i,j))] \geqslant t}{p}\right\} + \beta, \tag{5}$$

where α and β are constants, p is the mode of the corresponding image, t is the critical value, $\sum_{\text{mean}}(\text{particle}(Y(i,j)) \geqslant t)$ is the sum of mean Y values for the particles that exceed the critical value t in the corresponding image, and Y is the CIE tristimulus value. In addition, the particles were found by searching the eight connected region area with the pixel values that exceeded t in the image. The parameters α and β were obtained by minimizing the STRESS value of the measured glint value and the output of the glint prediction model of Eq. (5), as shown in Table 5. The STRESS value of 22 samples suggests that the output of the glint prediction model is highly consistent with the measured glint values given by the BYK mac[14−16].

Table 3. Augmented Matrices and the Sizes of Their Colorimetric Characterization Model for Digital Camera

Size	Augmented Matrices
3 × 9	$R\ G\ B\ RG\ RB\ GB\ R^2\ G^2\ B^2$
3 × 10	$R\ G\ B\ RG\ RB\ GB\ R^2\ G^2\ B^2\ 1$
3 × 11	$R\ G\ B\ RG\ RB\ GB\ R^2\ G^2\ B^2\ RGB\ 1$
3 × 20	$R\ G\ B\ RG\ RB\ GB\ R^2\ G^2\ B^2\ RGB\ R^2G\ R^2B\ G^2R\ G^2B\ B^2R\ B^2G\ R^3\ G^3\ B^3\ 1$
3 × 35	$R\ G\ B\ RG\ RB\ GB\ R^2\ G^2\ B^2\ RGB\ R^2G\ R^2B\ G^2R\ G^2B\ B^2R\ B^2G\ R^3\ G^3\ B^3\ R^3G\ R^3B\ G^3R$ $G^3B\ B^3R\ B^3G\ R^2GB\ RG^2B\ RGB^2\ R^2G^2\ R^2B^2\ G^2B^2\ R^4\ G^4\ B^4\ 1$

Table 4. Performance of the Characterization Models with Different Transfer Matrices

Size of Augmented Matrices	Median	Mean	Max	Min
3×9	2.45	2.76	8.31	0.40
3×10	2.01	2.10	5.01	0.38
3×11	1.65	1.85	4.48	0.24
3×20	0.93	1.09	3.76	0.23
3×35	0.49	0.46	1.42	0.01

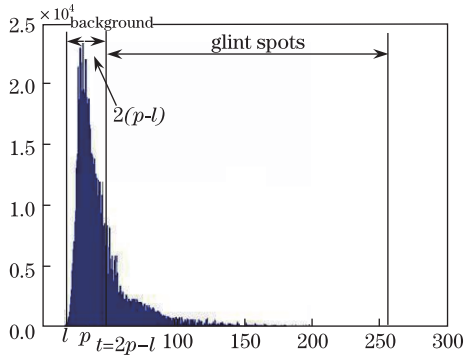

Fig. 3. Illustration of the distribution estimation method.

Table 5. Results of the Optimization for the Glint Prediction Model

α	β	STRESS
6.16	–21.49	22

Through the procedures above, the glint difference of each sample pair was calculated. The color difference of each sample pair was also predicted by employing the colorimetric characterization model for the camera. The total difference model could then be established, which was supposed to have a relationship with the color difference and the glint difference as

$$\Delta T = \sqrt{c_1(c_2\Delta L^{*2} + \Delta a^{*2} + \Delta b^{*2}) + c_3\Delta\mathrm{Glint}^2}, \quad (6)$$

where c_1, c_2, and c_3 are the constants to be optimized; ΔL^*, Δa^*, Δb^*, and ΔGlint are the color difference and glint difference, respectively; and ΔT is the visual total difference. For the optimization of Eq. (6), the STRESS values for the total difference of all sample pairs and the corresponding $\sqrt{c_1(c_2\Delta L^{*2} + \Delta a^{*2} + \Delta b^{*2}) + c_3\Delta\mathrm{Glint}^2}$ were minimized to determine the optimized values of c_i.

Similar to the camera characterization, an increase in the number of training samples could improve the model accuracy. Because of the limited amount of available samples for this study, only 36 of the 44 sample pairs were utilized as training sample pairs. The resulting constants c_i and the corresponding STRESS value of the training session are listed in Table 6. As seen from the table, c_2 is 1.06, which is very close to 1, suggesting that the lightness difference is of the same importance with the chromatic difference in the total difference for all the samples. The value of c_1(0.82) is less than c_3(2.55); meanwhile, it could not be concluded that the glint difference took greater part than the color difference in the total difference because of their different units.

Table 6. The Constants c_i of the Total Difference Model and the Corresponding STRESS Value

c_1	c_2	c_3	STRESS
0.82	1.06	2.55	24.8

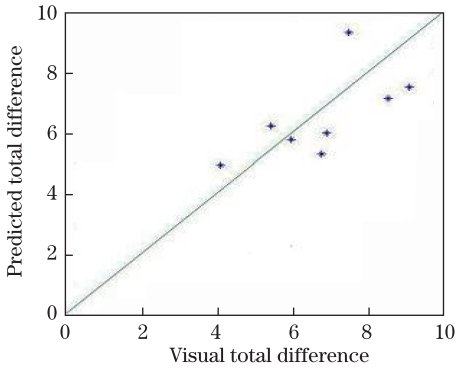

Fig. 4. Comparison between the total difference of the model output and the visual results.

Table 7. Model Performance in Terms of the Color Difference of CIELAB and STRESS

Max	Min	Mean	STRESS
1.82	0.20	1.13	18.6

The performance of the total difference model was evaluated using the remaining eight testing sample pairs, including two pairs of purple and green samples and one pair each of red, grey, blue, and yellow samples. The comparison between the predicted total difference by the model and the perceived total difference from the visual experiment is illustrated in Fig. 4. The scattered points are distributed evenly on both sides of the 45° ideal line, which indicated that the model accuracy is acceptable. The model performance, in terms of CIELAB color difference between the predicted total difference and the observed total difference and STRESS, also supports this conclusion; as shown in Table 7, the STRESS value is 18.6, which is even less than that of the model optimization. This might be because of the limited number of testing samples. The total difference model accuracy with a series of various ratios for training and testing sample pairs was also checked, and the results with ratio of 30:14, 25:19, and 20:24 were 2.56, 9.62, and 12.01 in terms of CIELAB color difference, respectively. It was evident that only the model accuracy with the training and testing sample pairs of the ratio (36:8) adopted in the study was close to 1 CIELAB color difference, whereas the others have values more than 1, implying that the balance between the training and testing sample pairs utilized in this study is suitable. The STRESS values of the model optimization and prediction were both small, indicating that the model proposed in this study could effectively predict the total difference of samples with metallic coating with high accuracy[14−16].

In conclusion, with the method of analyzing the images of the samples taken by a digital camera under the same illumination and viewing condition with the visual experiment, the color and glint information can

be quantized separately. The color difference and glint difference of the sample pairs can also be calculated; thus, the camera-based model is established to predict the total visual difference of the sample pairs under directional illumination. The input images for the model are taken under the viewing geometry that is identical to visual assessments such that the appearances of the samples can be accurately represented in the images. The testing results indicate that the camera-based model can precisely predict the total difference between samples with metallic coatings with satisfactory consistency to the corresponding visual data.

References

1. C. S. McCamy, Color Res. Appl. **21,** 292 (1996).
2. C. S. McCamy, Color Res. Appl. **23,** 362 (1998).
3. E. Kirchner, G.-J. van den Kieboom, L. Njo, R. Supèr, and R. Gottenbos, Color Res. Appl. **32,** 256 (2007).
4. N. Dekker, E. J. J. Kirchner, R. Supèr, G. J.van den Kieboom, and R. Gottenbos, Color Res. Appl. **36,** 4 (2011).
5. S. Kitaguchi, M. R. Luo, S. Westland, E. J. J. Kirchner, and G. J. van den Kieboom, in *Proceedings of 14th Color Imaging Conference Final Program and Proceedings* 197 (2006).
6. W. L. Chou, "Evaluation of lightness difference and metallic colour difference", PhD. Thesis (University of Derby, 2003).
7. S. Kitaguchi, "Modeling texture appearance of gonioapparent objects", PhD. Thesis (University of Leeds, 2008).
8. P. A. García, R. Huertas, M. Melgosa, and G. Cui, J. Opt. Soc. Am. A. **24,** 1823 (2007).
9. Z. Huang, H. Xu, M. R. Luo, G. Cui, and H. Feng, Chin. Opt. Lett. **8,** 717 (2010).
10. J. Y. Hardeberg, F. Schmitt, H. Brettel, J.-P. Crettez, and H. Maître, in *Colour Imaging: Vision and Technology* L.W. MacDonald and R. Luo, (eds.) (Wiley, 1999) P. 145.
11. G. Hong, M. R. Luo, and P. A. Rhodes, Color Res. Appl. **26,** 76 (2001).
12. K. Barnard and B. Funt, Color Res. Appl. **27,** 152 (2002).
13. M. R. Pointer, G. G. Attridge, and R. E. Jacobson, Imaging Sci. J. **49,** 63 (2001).
14. M. Melgosa, R. Huertas, and R. S. Berns, J. Opt. Soc. Am. A. **25,** 1828 (2008).
15. J. Ma, H. Xu, M. R. Luo, and G. Cui, Chin. Opt. Lett. **7,** 869 (2009).
16. J. Ma, "Colour quality assessment of inks on papers having different gloss levels", Master Thesis (in Chinese) (Zhejiang University, 2010).